Volcanic Eruptions in the Southern Red Sea During 2007–2013

Sigurjón Jónsson and Wenbin Xu

Abstract

The first volcanic eruption known to occur in the southern Red Sea in over a century started on Jebel at Tair Island in September 2007. The early phase of the eruption was energetic, with lava reaching the shore of the small island within hours, destroying a Yemeni military outpost and causing a few casualties. The eruption lasted several months, producing a new summit cone and lava covering an area of 5.9 km^2, which is about half the area of the island. The Jebel at Tair activity was followed by two more eruptions within the Zubair archipelago, about 50 km to the southeast, in 2011–2012 and 2013, both of which started on the seafloor and resulted in the formation of new islands. The first of these eruptions started in December 2011 in the northern part of the archipelago and lasted for about one month, generating a small (0.25 km^2) oval-shaped island. Coastal erosion during the first two years following the end of the eruption has reduced the size of the island to 0.19 km^2. The second event occurred in the central part of the Zubair Islands and lasted roughly two months (September–November, 2013), forming a larger (0.68 km^2) island. The recent volcanic eruptions in the southern Red Sea are a part of increased activity seen in the entire southern Red Sea region following the onset of a rifting episode in Afar (Ethiopia) in 2005.

Introduction

Several volcanic islands are located in the central part of the southern Red Sea between Yemen and Eritrea. The islands belong to Yemen and have been divided into three groups that from north to south are the Jebel at Tair Island, the Zubair group of islands, and the Hanish–Zukur Islands (Fig. 1). In addition, an older small and eroded volcanic island, called Perim, is located in the Strait of Mandeb (Bab-al-Mandab), between Yemen and Djibouti. Other islands in the southern Red Sea are located near the coastlines of Yemen, Saudi Arabia, and Eritrea, but not along the central axis of the Red Sea. These islands include the Farasan and Dahlak reef archipelagos (Fig. 1), located on Miocene sedimentary shelves (Almalki et al. 2014).

Jebel at Tair is a single, oval-shaped island, that is, ~11 km^2 in size and is for the most part covered by basaltic lava. The Zubair group contains just over 10 islands, most of which are small (<2 km in diameter), except the largest island (13 km^2), simply named Zubair Island. The Hanish–Zukur Islands are considerably larger and consist of three main islands, Zukur, and the great and little Hanish Islands, as well as several smaller islets and sea rocks. These islands are also primarily volcanic with evidence of both effusive and explosive activity. The three recent volcanic eruptions on Jebel at Tair and within the Zubair Islands during 2007–2008, 2011–2012, and 2013 were the first known eruptions to occur in the southern Red Sea for more than a century. Several eruptions were documented on Jebel at Tair and Zubair Islands during the eighteenth and nineteenth centuries (Siebert et al. 2010), but the most recent eruption within the Hanish–Zukur Islands is unknown.

The Tair and Zubair eruptions occurred in a remote and mostly uninhabited area where no seismometers or conventional geodetic instruments were installed to monitor volcanic and earthquake activity. Earthquakes located by

S. Jónsson (✉) · W. Xu
King Abdullah University of Science and Technology (KAUST), Thuwal 23955, Saudi Arabia
e-mail: sigurjon.jonsson@kaust.edu.sa

N.M.A. Rasul and I.C.F. Stewart (eds.), *The Red Sea*,
Springer Earth System Sciences, DOI 10.1007/978-3-662-45201-1_10,

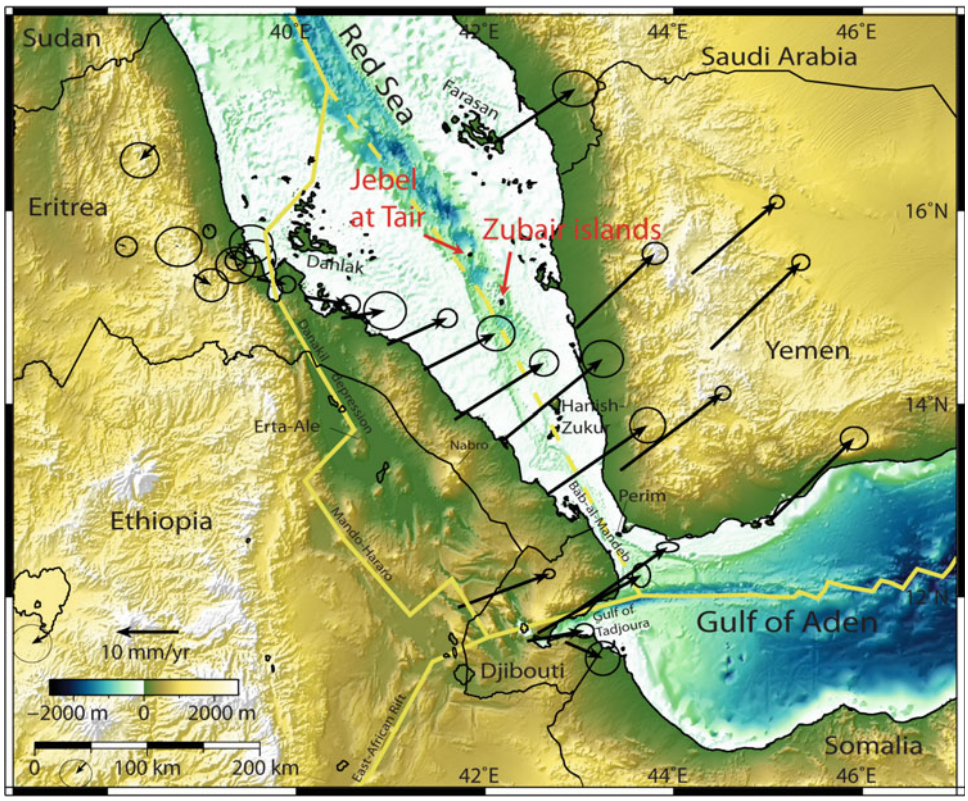

Fig. 1 Map of the southern Red Sea showing the location of Jebel at Tair and Zubair islands. Also shown are Farasan, Dahlak, Hanish–Zukur, and Perim islands and Erta Ale and Nabro volcanoes, GPS velocity vectors with error ellipses with respect to fixed Eurasia (ArRajehi et al. 2010), and plate boundaries (*yellow solid* and *dashed lines*)

regional networks provide limited information, although they show increased seismicity associated with the eruptions (International Seismological Centre 2013). Given the lack of local instrumental recordings and direct observations of the two eruptions, remotely sensed data from satellites provide key information for understanding and explaining the course of events during the eruptions and in the subsequent months. We therefore base our analysis of the volcanic activity on available medium- to high-resolution optical images as well as on images acquired by Synthetic Aperture Radar (SAR) instruments onboard several radar satellites.

Tectonic Background

The Red Sea has been opening since the Arabian plate broke away from the African plate about 24 million years ago (Bosworth et al. 2005). The rifting began with continental stretching and thinning and later progressed to sea-floor spreading. The rate of opening increases from about 7 mm/year in the northern Red Sea to roughly 16 mm/year in the south (ArRajehi et al. 2010; Reilinger et al. this volume). The rifting in the southern Red Sea is not focused on a single boundary, but is separated into two roughly parallel branches (Fig. 1). One branch follows the center of the Red Sea with a decaying opening rate toward the southeast until it dies out somewhere northwest of Mandeb Strait. The other branch follows the Danakil and Afar depressions in Eritrea and Ethiopia and meets up with the East African Rift and the Aden ridge in Djibouti to form a triple junction between the three rifts. GPS measurements show that the opening rate across the Danakil branch gradually increases to the southeast to the full rate between the Arabian and African plates (McClusky et al. 2010; Reilinger et al. this volume). This means that the area east of the Danakil depression and north of the Gulf of Tadjoura forms a separate tectonic block with the southern part of the block near the Mandeb Strait moving along with the Arabian Plate (Fig. 1). The central Red Sea trough becomes narrower and shallower from Jebel at Tair toward the Hanish–Zukur Islands, which is another manifestation of the decreasing opening rate of the Red Sea toward the southeast.

The region near the triple junction has been exceptionally active starting in 2005, with multiple earthquake swarms, volcanic eruptions, and magmatic intrusions. The Dabbahu rifting episode in the Manda-Hararo rift segment in Afar started in 2005 with a massive magma intrusion (Wright et al. 2006). It continued for several years with multiple earthquake swarms and intrusions (Grandin et al. 2010; Hamling et al. 2010). The rifting episode was preceded by an intrusion into the Dallol rift segment, north of Erta Ale volcano in the Danakil depression (Nobile et al. 2012). The Alu-Dalafilla volcano, also part of the Erta Ale volcanic range, erupted in 2008 and Nabro volcano in Eritrea erupted in 2011 (Smithsonian Institution 2008, 2011; Ogubazghi and

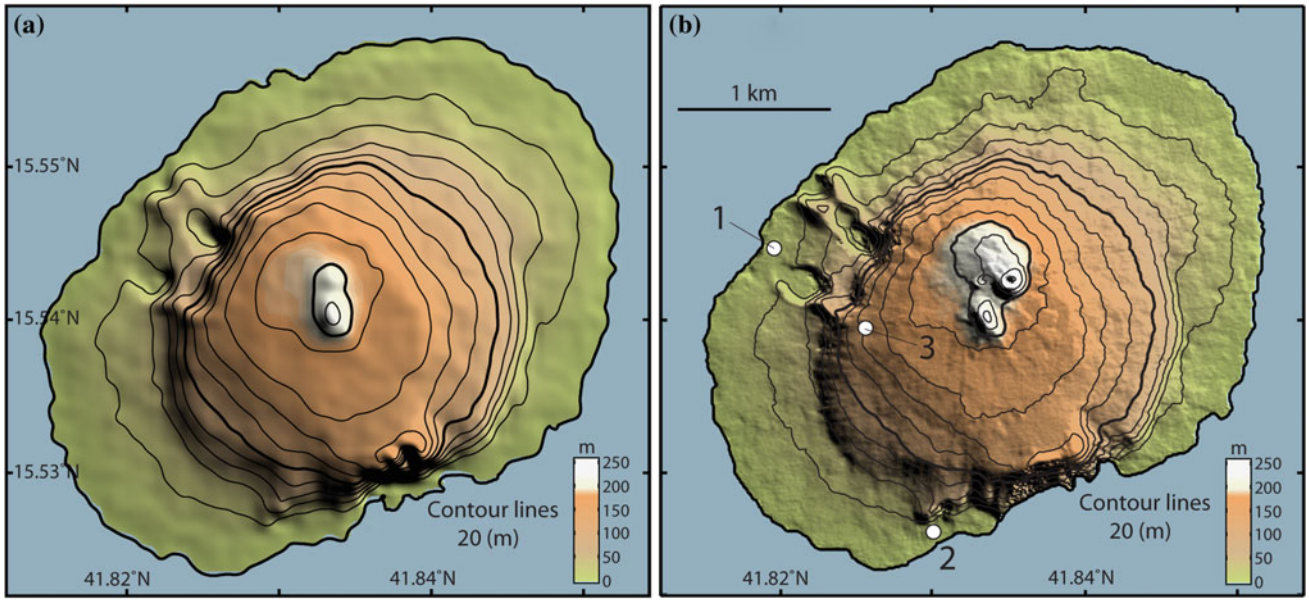

Fig. 2 Topographic maps of Jebel at Tair Island with 20-m contour lines from **a** interpolated SRTM and **b** TanDEM-X data. Numbers *1–3* in **b** indicate locations of buildings shown in Fig. 4

Goitom, this volume). In addition, an intensive earthquake swarm rocked the Gulf of Aden in November 2010 (Ahmed et al. 2012), and further north, an intrusion occurred in Harrat Lunayyir in western Saudi Arabia (Pallister et al. 2010). The three eruptions in the central Red Sea at Jebel at Tair and the Zubair Islands were a part of this general increase in volcanism across the region.

Jebel at Tair Island

The Jebel at Tair Island is located about 90 km from the Yemeni coastline, 120 km from Eritrea and 50 km northwest of the Zubair archipelago (Fig. 1). The island has an elliptical shape, about 4 km long and 3 km wide, covering an area of 11.4 km^2. It consists of a single stratovolcano and its highest point is 258 m above sea level. The volcanic edifice is significantly larger than that, as the average sea depth around the volcano is around 1,000 m, so the total height of the edifice exceeds 1,200 m.

We mapped the topography of the Jebel at Tair Island with satellite radar data from the TanDEM-X mission (Krieger et al. 2013). The TanDEM-X mission consists of two SAR satellites launched in 2007 (TerraSAR-X) and 2010 (TanDEM-X) that fly in a close formation, separated by only a few hundred meters, with one satellite transmitting X-band (3.1 cm) radar signals to the ground and both satellites receiving the reflected signals. With this bi-static configuration, a global digital elevation model (DEM) called WorldDEM is being produced that will be of unprecedented accuracy and coverage of the Earth's land surface (Rossi et al. 2012). We used TanDEM-X image pairs acquired on November 15, 2011 and December 26, 2012 with an incidence angle of ~34° from ascending orbits. Each image pair was precisely coregistered, and interferograms were formed by computing the phase difference between the two images. Then, we unwrapped the interferograms and generated height models, which we geo-referenced and averaged to produce a new DEM of the island (Fig. 2).

Our new TanDEM-X DEM provides much better information about the topography of the island than preexisting height models. The DEM pixel spacing is ~10 m, and the relative vertical accuracy of TanDEM-X DEMs is about 2 m (Krieger et al. 2013). In comparison, the posting of the Shuttle Radar Topography Mission (SRTM) DEM is only ~90 m (Farr et al. 2007) and the global ASTER GDEM around 30 m, but the ASTER GDEM includes only a part of Jebel at Tair Island. The improvement of the new TanDEM-X DEM can be clearly observed when displayed beside the SRTM DEM (here interpolated to 10 m posting) in Fig. 2. Note that the SRTM radar data were acquired in 2000, while the TanDEM-X was in 2011–2012, so the latter DEM includes the topographic changes that occurred as a result of the 2007–2008 eruption (see further analysis below).

The shape of Jebel at Tair Island is fairly symmetrical, with summit scoria cones and gentle slopes out to a radius of about 1 km, which are bounded by steeper slopes that again are surrounded by a gently sloping apron toward the coast. Gass et al. (1973) pointed out that this topographic profile indicates two separate periods of eruptive activity on Jebel at

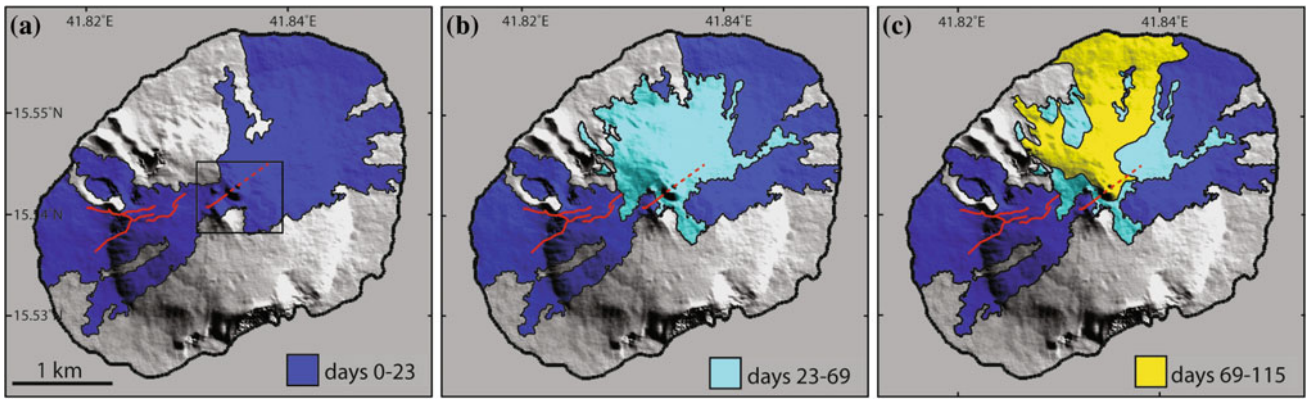

Fig. 3 Evolution of the 2007–2008 lava flow field on Jebel at Tair during the early (September 30, 2007–October 22, 2007), middle (October 23, 2007–December 8, 2007), and late (December 8, 2007–January 23, 2008) parts of the eruption. *Red lines* show eruptive fissures and the box in **a** marks the area covered in Fig. 6 (modified from Xu and Jónsson 2014a)

Tair with a significant dormant period between, during which sea cliffs formed. The sea cliffs are today mostly covered by lava from the second eruptive period, although they are still exposed on the southeastern side of the island.

Most of the surface of Jebel at Tair Island is covered by tholeiitic basaltic lava flows and is cut by numerous open radial fissures, possibly showing a slight orientation preference parallel to the trend of the Red Sea (Gass et al. 1973). Several historical eruptions are known to have occurred on Jebel at Tair before the 2007 activity, although the historical accounts for this region are neither long nor complete. There are reports of three eruptions during the nineteenth century, in 1833, 1863, and in 1883, and one in the eighteenth century, but no eruptions were recorded during the twentieth century (Siebert et al. 2010).

The 2007–2008 Jebel at Tair Eruption

The Jebel at Tair eruption started on September 30, 2007 and lasted at least until mid-January 2008 (Xu and Jónsson 2014a). The early phase of the eruption was energetic with lava extruding from fissures extending from the summit of the island toward both the west and the northeast. During this early phase, lava appears to have reached the shoreline within hours, as fresh lava extending to the sea could be seen during aerial inspection by Yemeni scientists on October 1, 2007 (Jamal M. Sholan, pers. comm. 2012). Lava was seen fountaining from a short fissure extending from the summit area and down to the northeastern flank of the volcano, while only steam was rising from fissures on the west flank. Lava fountaining during the later parts of the eruption was mostly confined within a new summit cone, with lava flowing to the north and to the northeast. The progress and coverage of the lava flow was analyzed by mapping interferometric decorrelation in a series of Interferometric Synthetic Aperture Radar (InSAR) images acquired by the Japanese ALOS satellite prior to, during and after the eruption (Xu and Jónsson 2014a). The total area of the new lava is 5.9 km^2, covering about 50 % of the island (Fig. 3).

Jebel at Tair was the site of a small Yemeni military outpost that was destroyed by the September 2007 eruption, resulting in several casualties (Smithsonian Institution 2007). Comparison between high-resolution (50–60 cm) optical images taken by the Quickbird and Worldview-2 satellites before and after the eruption shows damage and destruction of the military buildings (Fig. 4), with some surrounded or buried in lava, while others were probably damaged by tephra or earthquakes. The first images (Figs. 4a–b and 5) show a building near the northwest coast that was surrounded by the lava flow and with a collapsed roof. Another building, located on the south coast (Fig. 4c–d), was not threatened by the lava flows, but the collapsed roof suggests damage due to earthquake activity. Finally, a lighthouse (Fig. 4e–f), located halfway between the summit and the west coast, appears to have been completely destroyed by lava.

The high-resolution optical images from before and after the eruption reveal a number of other changes on the island (Xu and Jónsson 2014a). The pre-eruption image exhibits several radial fissures and a network of car tracks, which were partially buried by the 2007–2008 lava. The post-eruption images show that the coastline advanced by several tens of meters in a few places where lava flowed into the sea, particularly at the north coast, enlarging the area of the island by 0.13 km^2 (Xu and Jónsson 2014a). Changes in the summit area are especially pronounced, with a new prominent scoria cone and an underlying N60°E trending fissure, extending to the southwest and northeast of the cone (Figs. 5 and 6). This fissure clearly indicates the orientation of the dike feeding the eruption at the summit. More fresh fissures,

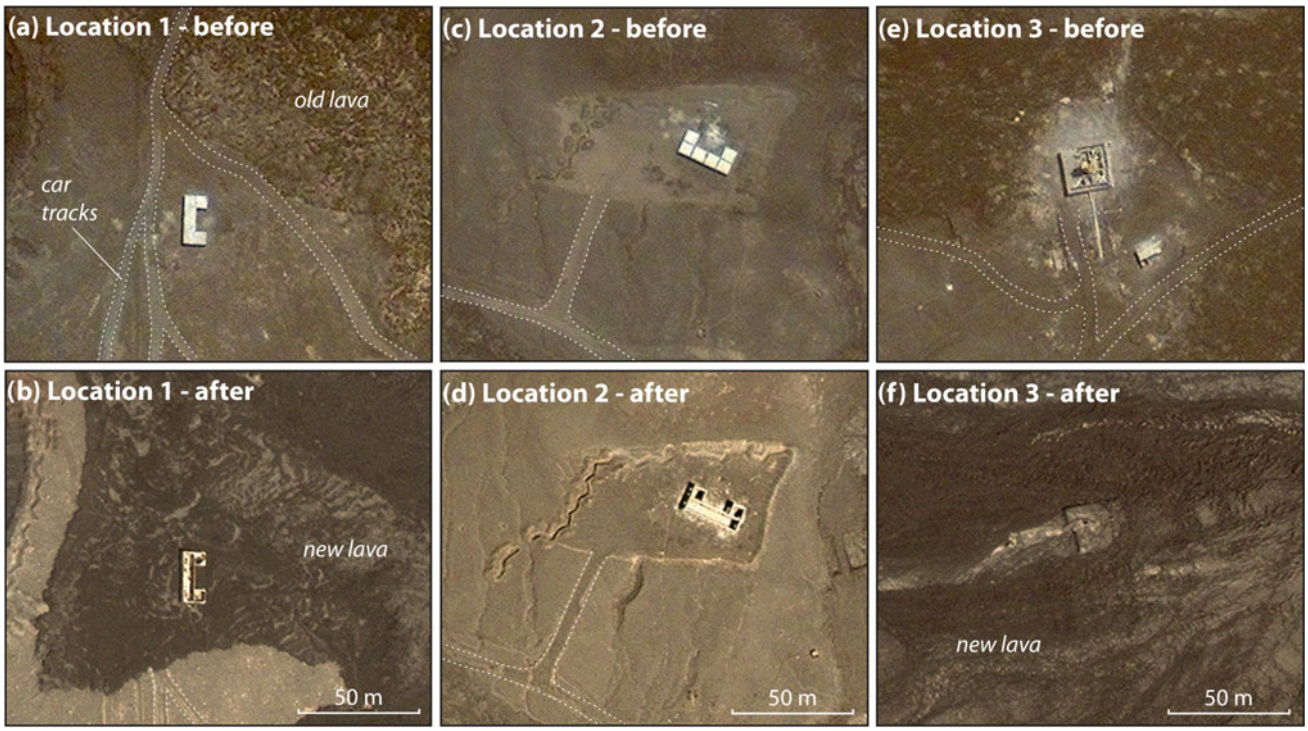

Fig. 4 Satellite optical image close-ups of buildings on Jebel at Tair before (*upper row*) and after (*lower row*) the 2007 eruption showing infrastructure damage caused by the volcanic activity. The locations of these three buildings are shown in Fig. 2, numbered *1–3*

Fig. 5 Photographs taken on Jebel at Tair on October 21, 2007, showing a building (*left*) surrounded by fresh lava (see also Fig. 4b) and the erupting summit cone (*right*). (*Photos* Jamal M. Sholan)

with more easterly strikes, can be seen in the post-eruption image further to the west. These fissures were active during the first hours of the eruption. The eruptive fissures also extended further to the northeast, as seen during the helicopter flight on October 1, 2007, but lava from the summit cone later buried them. Therefore, the total length of the eruptive fissures soon after the start of the eruption exceeded 1 km and may have been as long as 2 km, but quickly contracted to a short fissure during the first 24 h of activity. The eruption probably condensed to a single vent within days and continued there for over three months, building up the new summit scoria cone.

As we have DEMs of Jabel at Tair Island from before and after the 2007–2008 eruption (Fig. 2), we can estimate the thickness and volume of the eruptive products by differencing the two DEMs. However, the SRTM DEM is of much lower resolution and quality than the new TanDEM-X DEM, which makes this estimation somewhat inaccurate.

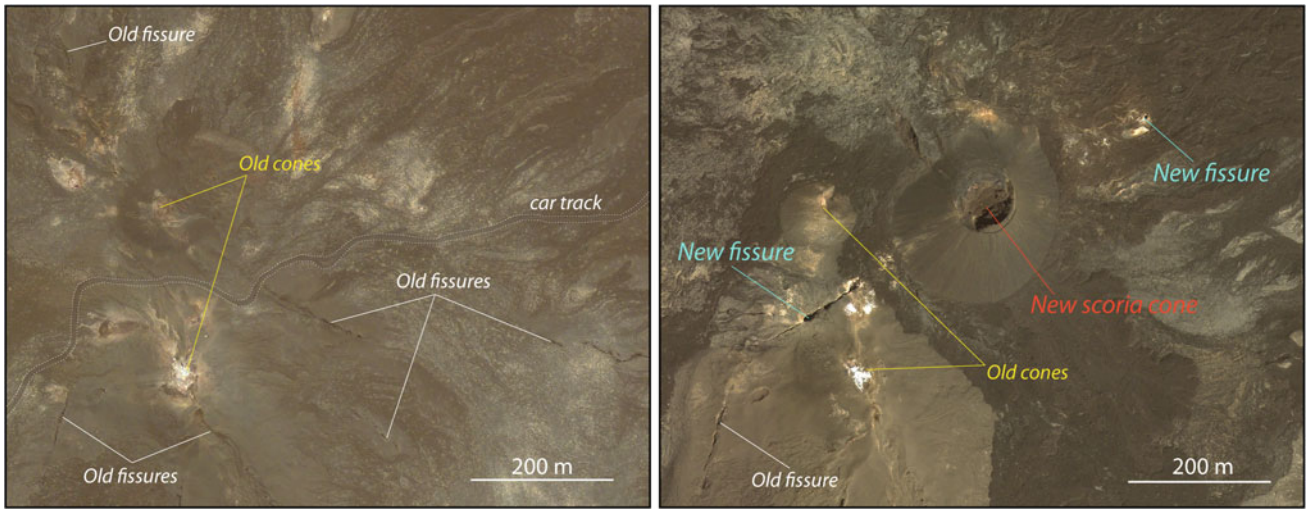

Fig. 6 Satellite optical image close-ups of the summit area of Jebel at Tair before (*left*) and after (*right*) the eruption showing eruptive fissures and a new summit scoria cone (the area covered in this figure is shown in Fig. 3a). The images were taken by the Quickbird (July 6, 2007) and Worldview-2 (October 22, 2011) satellites

We therefore used a series of pre-eruption InSAR data from the ALOS satellite to correct and improve the SRTM DEM (Xu and Jónsson 2014a). We then subtracted the ALOS-corrected SRTM from the new TanDEM-X DEM and produced a map of the height differences (Fig. 7). The height differences indicate that the average thickness of the lava is about 3.8 m, and the subaerial volume is 0.022 ± 0.011 km^3, or a dense-rock-equivalent (DRE) volume of ~ 0.017 km^3, assuming 25 % vesicularity (Xu and Jónsson 2014a). The uncertainty was estimated by comparing the height differences in areas that were not covered by the new lava; the standard deviation of the height differences in these areas is only 1.9 m. The volume estimate does not include the unknown amount of lava that flowed into the sea.

Comparison of satellite radar data from before and after the start of an eruption can be used to derive maps of the co-eruptive ground deformation in areas not covered by new lava flows. The main method is to form radar interferograms (InSAR) from pre- and post-eruption image pairs, where the interferometric phase provides information about the relative line-of-sight displacements between the ground and the radar satellites (Massonnet and Feigl 1998). In addition, offset tracking of features in radar amplitude images or optical images can be used to measure deformation if the displacements are large enough in comparison with the image resolution (Michel et al. 1999). We used InSAR data from both the Japanese ALOS and the European Envisat satellites to map co-eruptive ground displacements on Jebel at Tair along two different line-of-sight directions, as well as horizontal amplitude-image offsets (Xu and Jónsson 2014a). These different one-component displacement measurements,

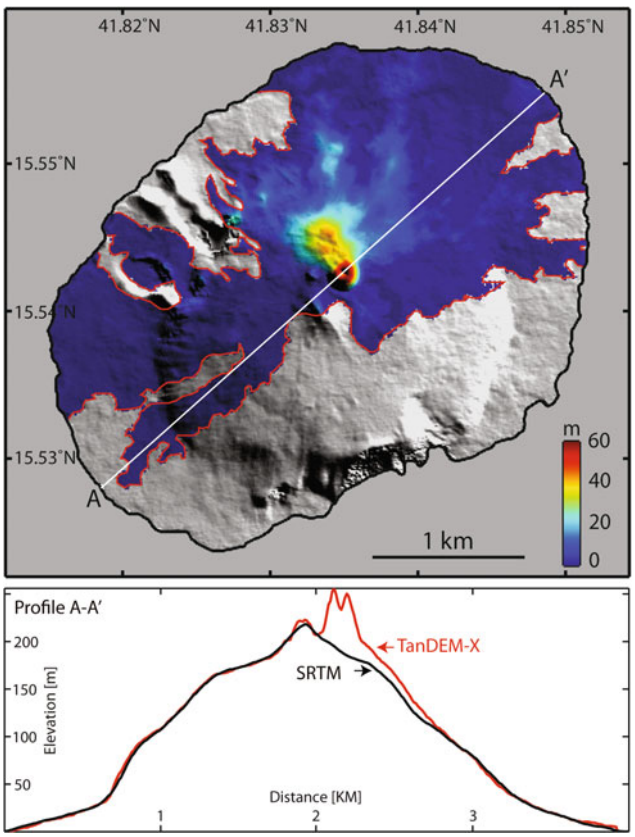

Fig. 7 The thickness of the 2007–2008 lava and other erupted deposits (*top*), estimated from the height differences between pre- and post-eruption DEMs (Fig. 2), see for example the DEM comparison along profile A–A′ (*bottom*) through the new summit cone (partly from Xu and Jónsson 2014a)

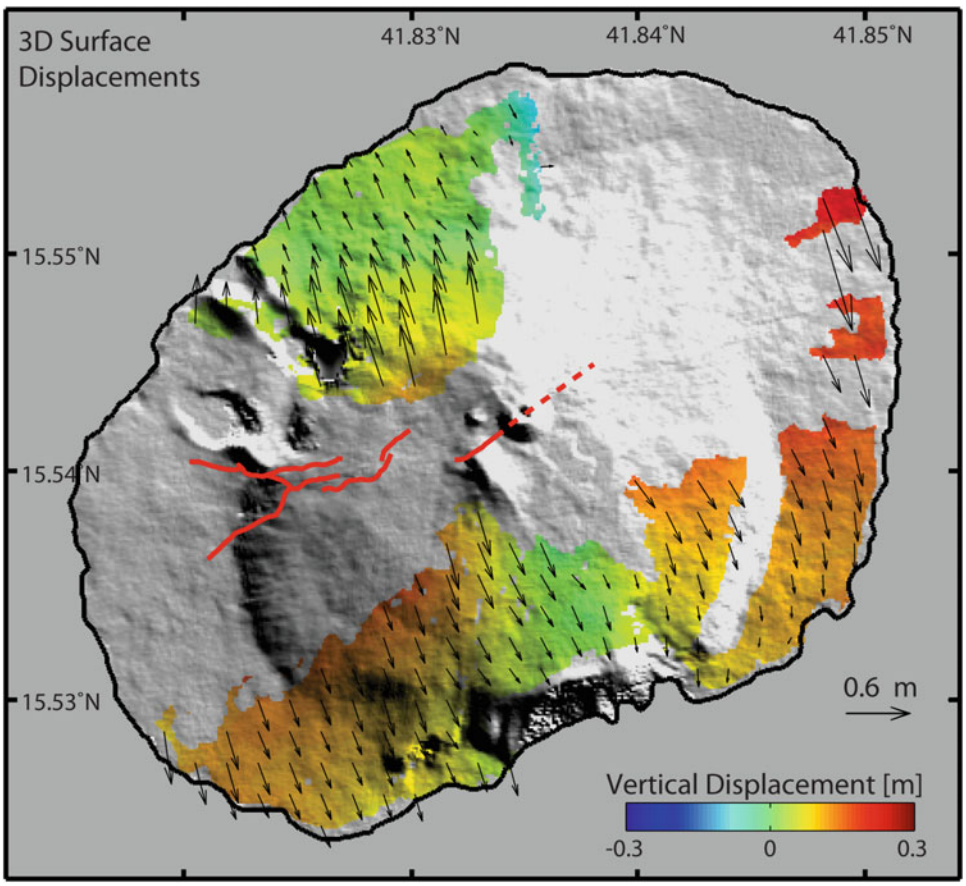

Fig. 8 Map of three-dimensional co-eruption surface displacements derived from satellite radar data, with arrows showing horizontal extension perpendicular to eruptive fissures (*red lines*) and colors indicating vertical movement

that is, the line-of-sight InSAR and the image-offset data, were then combined to invert three-dimensional (3D) displacements on the ground surface (Fig. 8). The map of the 3D deformation shows horizontal displacement of the northwest and southeast flanks of the volcano away from the eruptive fissures, with a maximum extension of over one meter. The vertical displacements are smaller and harder to interpret, although positive displacements (uplift) are seen near the intruding dike in most places. Modeling of this displacement field shows that a near-vertical dike, intersecting the surface at the mapped eruptive fissures, can roughly explain the observed deformation (Xu and Jónsson 2014a).

The northeast orientation of the feeder dike is surprising as it is roughly perpendicular to the axis of the Red Sea rift. Older surface fissures are easily identified in satellite images from before the 2007–2008 eruption, and they exhibit several different radial directions (Gass et al. 1973; Xu and Jónsson 2014a). This indicates that the stress field within the Jebel at Tair volcanic edifice is both isolated from the regional Red Sea stress field and that it has varied with time. Each new dike intrusion seems to modify the local stress field enough such that the next intrusion ascends to the surface with a different orientation. Comparable temporal variations of stress orientations within other volcanoes have recently been found, for example on Fernandina volcano, Galápagos (Chadwick et al. 2011).

Zubair Islands

The Zubair archipelago is located about 50 km southeast of Jebel at Tair, about 50 km from the Yemeni coast and just over 100 km from Eritrea (Fig. 1). These islands are sitting on a shallow (<100 m) north-northwest-oriented platform, that is, ~25 km long and ~10 km wide. The platform is situated within the Red Sea median trough and is separated from the trough flanks by narrow trenches to the west and to the east, which are up to 900 m deep (Gass et al. 1973). Before the 2011–2013 activity, the archipelago consisted of 10 small islands and several sea rocks. The largest island, simply called Zubair Island, is about 5 km long, 3 km wide and covers an area of ~13 km^2. The other islands are significantly smaller, mostly less than 2 km in diameter (Fig. 9). The dominant structural trend found on some of the islands, for example on Zubair Island, is ~N10°W (Gass et al. 1973), or similar to the overall north-northwest orientation of the entire archipelago and the Red Sea rift.

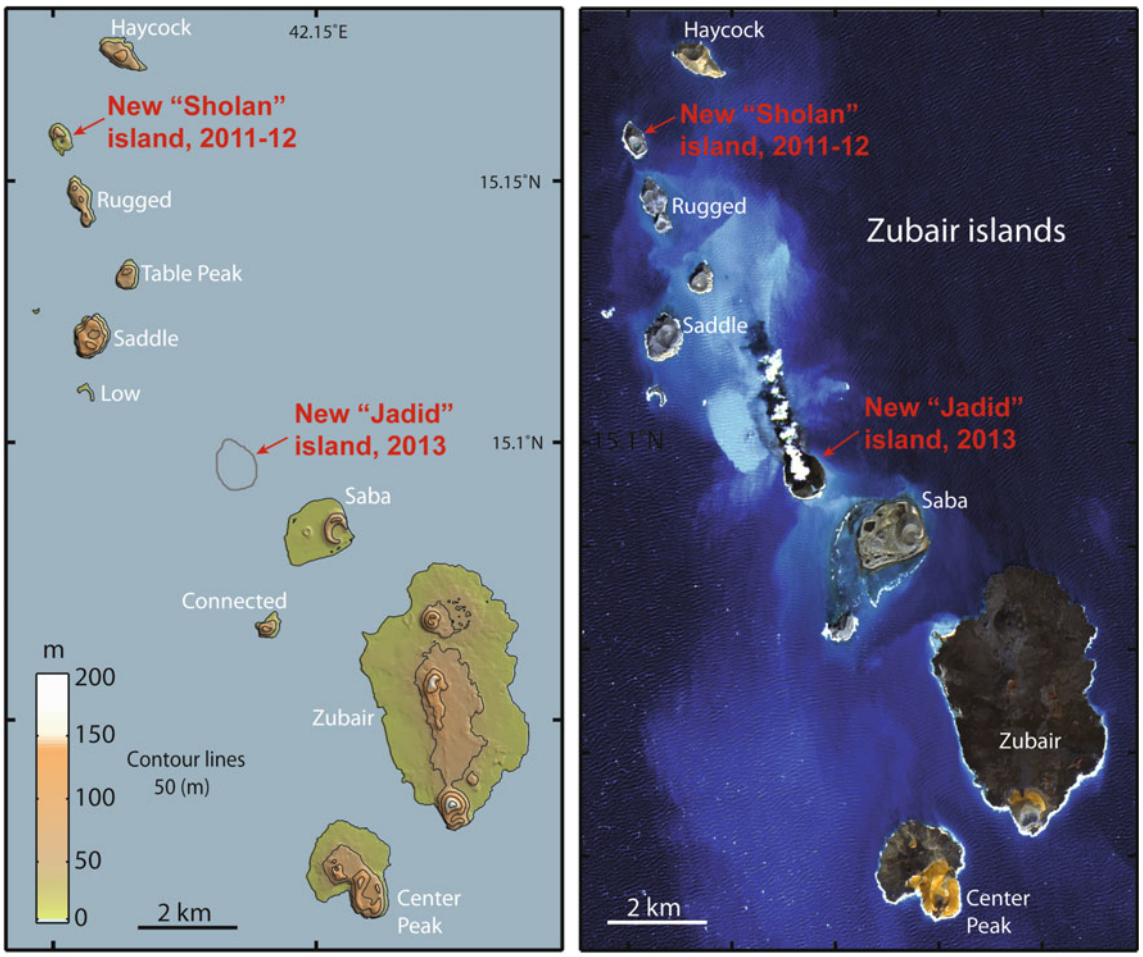

Fig. 9 Topographic map (*left*) of the Zubair archipelago (generated from TanDEM-X data) showing the location of the new islands (Sholan and Jadid) formed during the 2011–2012 and 2013 eruptions. The Landsat-8 image (*right*) is from Nov 8, 2013 and shows steam and ash rising from the new Jadid Island in the central part of the archipelago. The map does not include Quoin Island, which is also considered a part of the archipelago but is located off the map to the northwest

The Zubair Islands are all of volcanic origin and primarily consist of basaltic tuff, agglomerate, and lava (Gass et al. 1973). They were formed in surtseyan eruptions that started as submarine activity and then progressed to explosive phreatomagmatic eruptions, building up a ring of agglomerates and ash. In some cases, the activity developed to a point at which the tuff ring protected the eruptive vent from the seawater, allowing for transition to an effusive lava eruption, similar to that observed during the 1963–1967 Surtsey eruption south of Iceland (Moore 1985). This is evident on Zubair and Centre Peak Islands where lava covers a significant portion of their exposed surfaces (Fig. 9). In other cases, the activity did not progress beyond the explosive phase, such as on Rugged, Saddle, and Connected Islands (Gass et al. 1973), as well as on some other small islands and sea rocks.

There is also evidence for a period of quiescence on some of the islands, separating two phases of eruptive activity (Gass et al. 1973). In these cases, on Centre Peak, Saba, and Zubair Islands, the earlier phase eruptions all progressed to effusive activity, producing lava near the original vent. The activity in the later phase produced scoria cones and more lava. The quiescence is marked by erosional sea cliffs that are in many places covered by volcanic products from the second phase.

Similar to Jebel at Tair, the historical accounts of eruptions are limited and many eruptions may have occurred unnoticed, especially before the opening of the Suez Canal in 1869. Two eruptions are known to have occurred within the Zubair Islands before the recent activity began. Both of them are reported to have taken place on Saddle Island during the nineteenth century, in 1824 and in 1846 (Siebert et al. 2010), although the latter one is classified as uncertain.

The 2011–2012 Zubair Eruption

Yemeni fishermen reported an offshore eruption near the Zubair Islands on December 18, 2011. The surtseyan eruption occurred in shallow seawater between Haycock and Rugged Islands (Fig. 9), and by December 23, 2011, a new island (Sholan Island) had formed at the eruption site. The exact timing of the onset of the eruption is not known. Two earthquakes of magnitude 3.7 and 3.9 occurred on 13 December, and the eruption may have started on the seafloor following these events. However, there are no signs of the activity in satellite images until on 18 December, when a clear plume is seen rising from the eruption site (Smithsonian Institution 2013).

The eruption appears to have started along a short north-northwest-oriented fissure, parallel to the dominant structural trends of the archipelago, as indicated by the elongated activity seen on the satellite image from December 23, 2011 (Fig. 10a). Later, the eruption was restricted to a single vent and continued well into January (Xu and Jónsson 2014b). Strong phreatomagmatic activity can be seen in a video, taken on January 2, 2012 from a Yemeni military helicopter, sending a significant amount of tephra into the sky. The end of the eruption was reported as sometime between January 7, 2012 and January 15, 2012 (Smithsonian Institution 2013). However, high-resolution images taken by the Worldview-2 satellite can further constrain the end of the activity, as an image from January 9, 2012 shows that the eruption was still ongoing but had ended by January 12, 2012 (Fig. 10). Given this information, as well as a MODIS thermal anomaly that was detected on January 11, 2012 at 22:35 UTC (Smithsonian Institution 2013), we time the end of the eruption to the early morning of January 12, 2012. The duration of the subaerial activity was thus 25 days, from December 18, 2011 to January 12, 2012.

The eruption did not progress beyond an explosive phase. The satellite image from January 9, 2012 shows that seawater is in contact with the eruptive vent from the southwest and that explosive activity is still ongoing (Fig. 10b). In addition, no effusive eruption products can be seen in the January 12, 2012 image, immediately after the end of the eruption (Fig. 10c). The new Sholan Island is therefore similar to many of the smaller Zubair Islands that were likely also formed in single explosive eruptions, which probably lasted days to weeks, rather than months to years.

The January 12, 2012 image shows that Sholan Island was about 0.77 km long and 0.52 km wide at the end of the eruption, covering an area of 0.25 km^2 (Xu et al. 2015).

Fig. 10 Series of high-resolution images from the Quickbird and Worldview-2 satellites of the new Sholan Island in the northern Zubair archipelago, showing the 2011–2012 eruption and post-eruptive coastal changes

Fig. 11 Photograph of Sholan Island in the northern Zubair archipelago, taken from the southeast on January 17, 2012 (*photo* Jamal M. Sholan)

Images from subsequent months show how the shape and size of the island changed due to coastal erosion and landslides. This erosion and evidence for landslide activity can be seen in a photograph of the island taken shortly after the end of the eruption (Fig. 11). By March 2012, notable changes to the island's shape had already taken place and a lake had formed in the main crater (Fig. 10d). Further coastal changes can be seen in the June 2012 image (Fig. 10e) with the area of Sholan Island reduced to $\sim$0.24 km^2, and then to $\sim$0.19 km^2 by the end of 2013, or to about 75 % of its size at the end of the eruption.

The 2013 Zubair Eruption

A new volcanic eruption started in the Zubair archipelago on September 28, 2013, when a steam plume and a clear SO_2 anomaly were detected from satellite data (NASA-OMI 2013). The exact start time of the eruption is unknown, but no subaerial activity is visible in satellite images collected on and before September 27, 2013. No earthquakes were detected before or during this activity by stations in Yemen or Eritrea (International Seismological Centre 2013).

This eruption took place further south than the 2011–2012 eruption, between Saddle and Saba Islands (Fig. 9). Within days, a new island (Jadid Island) had formed about 2 km northwest of Saba Island, and the island grew larger as the eruption continued through October and into November. As with the onset of the eruption, the timing of the eruption's end can only be constrained by satellite data. A plume is seen rising from the island in a Landsat-7 image on November 16, 2013 (Fig. 12d), but no activity is visible in a Landsat-8 image from November 24, 2013 (Fig. 12e). Furthermore, MODIS data seem to indicate a small thermal anomaly on 20 November, but no anomaly is seen in the MODIS data from 21 November (NASA-MODIS 2013). We therefore estimate the end of the eruption between these two days and its total duration is $\sim$54 days, which is more than twice as long as the 2011–2012 eruption.

The new Jadid Island is also significantly larger than Sholan Island formed during the 2011–2012 eruption; it is about 0.9 km in diameter, with an area of $\sim$0.68 km^2 (Xu et al. 2015). However, similar to the earlier activity, the eruption does not seem to have progressed beyond an explosive phase to an effusive phase, as satellite images late in the eruption, for example on November 8, 2013 and November 16, 2013 (Fig. 12c–d), indicate only explosive activity. In addition, medium-resolution satellite images from after the eruption do not show signs of lava on the new island, although this has yet to be confirmed by field inspection or higher resolution imagery.

Discussion and Conclusions

The Jebel at Tair and Zubair volcanic eruptions occurred in a remote offshore and mostly uninhabited area without seismometers or conventional geodetic instruments. Only three brief visits were paid to the islands by Yemeni scientists during the eruptions, and these were the only direct observations, along with occasional photographs and videos (posted on the Internet) from ships passing by or from Yemeni military personnel. Almost all the information we have about this activity is from optical and radar satellite images, highlighting the importance of remote sensing in detecting, monitoring, and understanding offshore and remote volcanic activity.

Earthquakes located by regional networks provide only limited information, although they show increased seismicity near Jebel at Tair Island as early as September 21, 2007 (International Seismological Centre 2013), nine days before the eruption started. At least four $M_L > 4$ earthquakes occurred during the afternoon of September 30, 2007, which probably coincided with the dike propagating to the surface. Limited earthquake activity was recorded before the 2011–2012 and

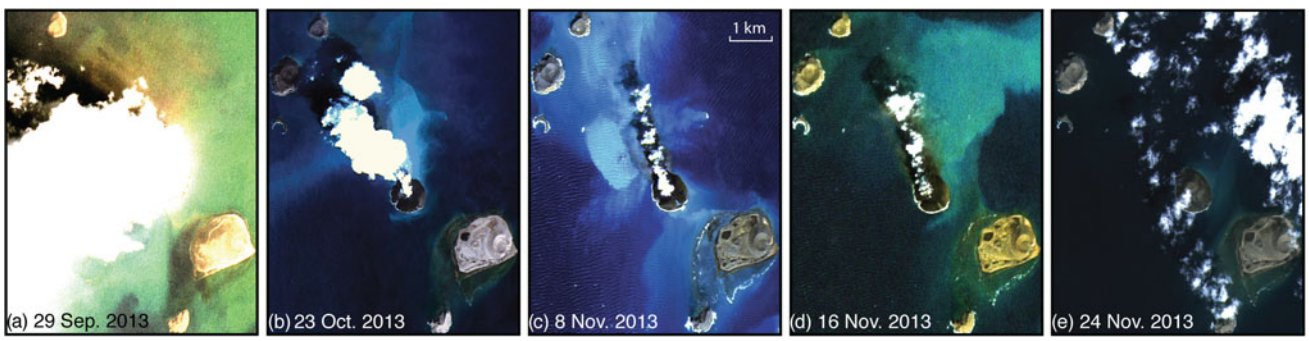

Fig. 12 A series of satellite images of the new Jadid Island in the central part of the Zubair archipelago, showing the 2013 eruption and post-eruptive changes. The images are from the Landsat-7 and Landsat-8 satellites

2013 Zubair eruptions. Only two earthquakes were detected in the area several days before the 2011–2012 eruption started, and no recorded earthquakes coincided with the start of the 2013 eruption. The lack of pre-eruption earthquakes is due to the limited monitoring capability of the current seismic stations, located more than 100 km away on the Yemeni mainland. Therefore, improved seismic monitoring with seismic stations on the islands in the southern Red Sea is needed to forecast and monitor future eruptions.

The eruptions on Jebel at Tair in 2007–2008 and within the Zubair archipelago in 2011–2012 and 2013 were the first eruptions in the southern Red Sea for more than a century. The Zubair Islands had only two known eruptions prior to the 2011–2012 and 2013 activity, according to historical accounts, in 1824 and in 1846, while four previous eruptions are reported on Jebel at Tair, in ~1750, 1833, 1863, and 1883 (Siebert et al. 2010). The reawakening of eruptive activity in the Red Sea coincides with increased volcanic activity across the entire region that started with the large Dabbahu diking event in Afar in 2005 (Wright et al. 2006). Since then, multiple dike intrusions and several eruptions have occurred in Afar, the Red Sea, and the Gulf of Aden (e.g., Hamling et al. 2010; Smithsonian Institution 2008, 2011; Ahmed et al. 2012). While it is not clear how these events are related to one another, the burst of activity since 2005 strongly suggests that there is a link between them. Mapping of transient crustal strain caused by the initial diking event and subsequent dike intrusions in the Dabbahu rifting episode shows that significant strain extends hundreds of kilometers away from the Manda-Hararo rift segments and affects the southern Red Sea and Gulf of Aden (Pagli et al. 2012). While the exact nature of the stress changes caused by the Dabbahu rifting episode in the southern Red Sea islands has not yet been studied in detail, strong stress changes with influence on earthquake occurrence have been reported far away from other rifting episodes (Maccaferri et al. 2013), thus demonstrating the potential for a connection between the Red Sea eruptions and the distant Dabbahu activity.

Acknowledgments We thank Jamal M. Sholan (Seismological and Volcanological Observation Center, Dhamar, Yemen) for providing field photos and information about the Jebel at Tair and Zubair activity. We have named the two new islands in the Zubair archipelago Jadid ("new" in Arabic) and Sholan, as Jamal Sholan was the first Yemeni scientist to visit that island. The Envisat and ERS satellite data were provided by the European Space Agency (ESA) and ALOS data by the Japan Exploration Agency (JAXA) through Category-1 Project #6703. The German Space Agency provided the TanDEM-X data through project XTI-GEOL3441. The Landsat-7 and 8 images were distributed by the Land Processes Distributed Active Archive Center (LP DAAC), located at USGS/EROS, Sioux Falls, SD (http://lpdaac.usgs.gov). The research reported in this publication was supported by King Abdullah University of Science and Technology (KAUST).

References

Ahmed A, Doubre C, Leroy S, Perrot J, Audin L, Rolandone F, Keir D, Al-Ganad I, Khanbari K, Mohamed K, Vergne J, Jacques E, Nercessian A (2012) November 2010 earthquake swarm—western Gulf of Aden (abstract). In: Proceedings of the Afar Rift Consortium conference, Addis Ababa, Ethiopia, 11–13 Jan 2012

Almalki KA, Betts PG, Aillers L (2014) Episodic sea-floor spreading in the Southern Red Sea. Tectonophysics 617:140–149

ArRajehi A, McClusky S, Reilinger R, Daoud M, Alchalbi A, Ergintav S, Gomez F, Sholan J, Bou-Rabee F, Ogubazghi G, Haileab B, Fisseha S, Asfaw L, Mahmoud S, Rayan A, Bendik R, Kogan L (2010) Geodetic constraints on present-day motion of the Arabian Plate: Implications for Red Sea and Gulf of Aden rifting. Tectonics 29: TC3011, doi:10.1029/2009TC002482

Bosworth W, Huchon P, McClay K (2005) The Red Sea and Gulf of Aden Basins. J Afr Earth Sci 43:334–378

Chadwick WW, Jónsson S, Geist DJ, Poland M, Johnson DJ, Batt S, Harpp KS, Ruiz A (2011) The May 2005 eruption of Fernandina volcano, Galapagos: GPS and InSAR observations of a circumferential dike intrusion. Bull Volc 73:679–697

Farr TG, Rosen PA, Caro E, Crippen R, Duren R, Hensley S, Kobrick M, Paller M, Rodriguez E, Roth L, Seal D, Shaffer S, Shimada J, Umland J, Werner M, Oskin M, Burbank D, Alsdorf D (2007) The Shuttle Radar Topography Mission. Reviews of Geophysics 45: RG2004, doi:10.1029/2005RG000183

Gass IG, Mallick DIJ, Cox KG (1973) Volcanic islands of the Red Sea. J Geol Soc Lond 129(3):275–309

Grandin R, Socquet A, Jacques E, Mazzoni N, de Chabalier J-B, King GCP (2010) Sequence of rifting in Afar, Manda-Hararo rift, Ethiopia, 2005–2009: Time-space evolution and interaction between dikes from Interferometric synthetic aperture radar and static stress change modeling. J Geophys Res 115:B10413. doi:10.1029/2009JB000815

Hamling IJ, Wright TJ, Calais E, Bennati L, Lewi E (2010) Stress transfer between thirteen successive dyke intrusions in Ethiopia. Nat Geosci 3:713–717

International Seismological Centre (2013) On-line Bullet, International Seismological Centre, Thatcham. http://www.isc.ac.uk

Krieger G, Zink M, Bachmann M, Bräutigam B, Schulze D, Martone M, Rizzoli P, Steinbrecher U, Antony JW, De Zan F, Hajnsek I, Papathanassiou K, Kugler F, Cassola MR, Younis M, Baumgartner S, López-Dekker P, Prats P, Moreira A (2013) TanDEM-X: a radar interferometer with two formation-flying satellites. Acta Astronaut 89:83–98

Maccaferri F, Rivalta E, Passarelli L, Jónsson S (2013) The stress shadow induced by the 1975–1984 Krafla rifting episode. J Geophys Res 118:1109–1121

Massonnet D, Feigl KL (1998) Radar interferometry and its application to changes in the Earth's surface. Rev Geophys 36:441–500

McClusky S, Reilinger R, Ogubazghi G, Amleson A, Healeb B, Vernant P, Sholan J, Fisseha S, Asfaw L, Bendick R, Kogan L (2010) Kinematics of the southern Red Sea-Afar Triple Junction and implications for plate dynamics. Geophys Res Lett 37:L05301. doi:10.1029/2009GL041127

Michel R, Avouac JP, Taboury J (1999) Measuring ground displacements from SAR amplitude images: application to the Landers earthquake. Geophys Res Lett 26:875–878

Moore JG (1985) Structure and eruptive mechanisms at Surtsey Volcano, Iceland. Geol Mag 122:649–661

NASA-MODIS 2013, The MODIS website. http://modis.gsfc.nasa.gov

NASA-OMI 2013, Global sulfur monitoring home page. http://so2.gsfc.nasa.gov

Nobile A, Pagli C, Keir D, Wright TJ, Ayele A, Ruch J, Acocella V (2012) Dike-fault interaction during the 2004 Dallol intrusion at the northern edge of the Erta Ale Ridge (Afar, Ethiopia). Geophys Res Lett 39:L19305. doi:10.1029/2012GL053152

Pagli C, Wright TJ, Wang H, Calais E, Bennati L, Lewi E (2012) Three-dimensional time-varying crustal velocity and strains in the Afar triangle. In: Proceedings of the Afar Rift Consortium conference, Addis Ababa, Ethiopia, 11–13 Jan 2012

Pallister JS, McCausland WA, Jónsson S, Lu Z, Zahran HM, El-Hadidy S, Aburukbah A, Stewart ICF, Lundgren PR, White RA, Moufti MRH (2010) Broad accommodation of rift-related extension recorded by dyke intrusion in Saudi Arabia. Nat Geosci 3:705–712

Rossi C, Gonzalez FR, Fritz T, Yague-Martinez N, Eineder M (2012) TanDEM-X calibrated raw DEM generation. ISPRS J Photogram Remote Sens 73:12–20

Siebert L, Simkin T, Kimberly P (2010) Volcanoes of the world (3rd ed). Smithsonian Institution, University California Press, Oakland, 551 pp

Smithsonian Institution (2007) Jebel at Tair. In: Bulletin of the global volcanism network, 32(10):2−5

Smithsonian Institution (2008) Jebel at Tair. In: Bulletin of the global volcanism network, 33(4):11−12

Smithsonian Institution (2011) Zubair. Bulletin of the global volcanism network, 36(11):2−4

Smithsonian Institution (2013) Zubair. In: Bulletin of the global volcanism network, 38(4):17−18

Wright TJ, Ebinger C, Biggs J, Ayele A, Yirgu G, Keir D, Stork A (2006) Magma-maintained rift segmentation at continental rupture in the 2005 Afar dyking episode. Nature 442:291–294

Xu W, Jónsson S (2014a) The 2007–2008 volcanic eruption on Jebel at Tair island (Red Sea), observed by satellite radar and optical images. Bull Volc 76:1−14. doi: 10.1007/s00445-014-0795-9

Xu W, Jónsson S (2014b) Two recent surtseyan eruptions in the Zubair archipelago (Red Sea) studied using high-resolution radar and optical satellite remote sensing. Geophysical Research Abstracts, vol 16, EGU2014-1224-1

Xu W, Ruch J, Jónsson S (2015) Birth of two volcanic islands in the southern Red Sea (in revision)